The fetal origin of adult atherosclerosis : a study in ApoE and Ldlr mouse models

Alkemade, F.E.

Chapter 2

Intrauterine Exposure to Maternal Atherosclerotic Risk Factors Increases the Susceptibility to Atherosclerosis in Adult Life

Fanneke E. Alkemade[1], Adriana C. Gittenberger-de Groot[1], Anja E. Schiel[2], J. Conny VanMunsteren[1], Bianca Hogers[1], Leontien S.J. van Vliet[1], Louis M. Havekes[3,4,5], Ko Willems van Dijk[2,3], Marco C. DeRuiter[1]

[1]Department of Anatomy and Embryology, [2]Department of Human Genetics, [3]Department of General Internal Medicine, [4]Department of Cardiology, Leiden University Medical Center, Leiden, The Netherlands; [5]TNO-Quality of Life, Gaubius Laboratory, Leiden, The Netherlands

Modified after Arteriosclerosis Thrombosis and Vascular Biology 2007;27:2228-2235

Intrauterine Exposure to Maternal Atherosclerotic Risk Factors Increases the Susceptibility to Atherosclerosis in Adult Life

Abstract

Maternal hypercholesterolemia is associated with a higher incidence and faster progression of atherosclerotic lesions in neonatal offspring. We aimed to determine whether an in utero environment exposing a fetus to maternal hypercholesterolemia and associated risk factors can prime the murine vessel wall to accelerated development of cardiovascular disease in adult life. To investigate the epigenetic effect in utero, we generated genetically identical heterozygous apolipoprotein E-deficient progeny from mothers with a wild-type or apolipoprotein E-deficient background. A significant increase in loss of endothelial cell volume was observed in the carotid arteries of fetuses from apolipoprotein E-deficient mothers, but fatty streak formation was absent. Spontaneous atherosclerosis development was absent in the aorta and carotid arteries in adult life. We unilaterally placed a constrictive collar around the carotid artery to induce lesion formation. In offspring from apolipoprotein E-deficient mothers, collar placement resulted in severe neointima formation in 9 of 10 mice analyzed compared with only minor lesion volume (2 of 10) in the progeny of wild-type mothers. We conclude that the susceptibility to neointima formation of morphologically normal adult arteries is already imprinted during prenatal development and manifests itself in the presence of additional atherogenic risk factors in adult life. Future research will concentrate on the mechanisms involved in this priming process, as well as on prevention strategies.

Introduction

Postnatal risk factors of atherosclerosis are well-defined and mechanisms contributing to lesion formation are increasingly understood. Previous studies showed that the atherogenic process in humans can already start during fetal development.[1] In a morphometric postmortem analysis of atherosclerosis in fetuses and children (Fate of Early Lesions in Children Study),[2] it was demonstrated that specifically maternal hypercholesterolemia was associated with a higher incidence of atherosclerotic lesions during the fetal period and a faster progression of these atherosclerotic lesions after birth, even under conditions of normocholesterolemia in the offspring. A causal role for maternal hypercholesterolemia in fetal lesion formation was demonstrated in a genetically nonhomogeneous rabbit model of diet-induced hypercholesterolemia and confirmed in a low-density lipoprotein receptor-deficient mouse model ($Ldlr^{-/-}$).[3,4] Raised cholesterol intake of pregnant $Ldlr^{-/-}$ mice accelerated the progression of spontaneous atherosclerotic lesions in the $Ldlr^{-/-}$ progeny. Because these mice have elevated plasma cholesterol levels independent of the maternal cholesterol levels during postnatal life, they are genetically prone to develop atherosclerotic lesions. The question remains whether solely environmental atherogenic risk factors present in utero can prime the developing vascular system.

We hypothesized that the offspring without a genetic predisposition for spontaneous atherosclerosis, which had been exposed in utero to maternal atherosclerotic risk factors, would show increased susceptibility for atherosclerosis development in adult life compared with offspring from wild-type mothers. To solely investigate the epigenetic effect, we generated genetically identical heterozygous apolipoprotein E-deficient mice ($apoE^{+/-}$) from mothers with a normocholesterolemic wild-type or a hypercholesterolemic apoE-deficient ($apoE^{-/-}$) background and studied the morphology of the carotid arteries during the fetal and adult period. Homozygous apoE-deficiency is associated with hypercholesterolemia and spontaneous development of extensive atherosclerosis resembling human lesion composition.[5,6] $ApoE^{+/-}$ mice on the other hand, only develop hypercholesterolemia and atherosclerosis when fed a high-fat Western-type diet.[7,8] To study the effect of maternal atherosclerotic risk factors in utero, we examined the morphology of the vascular wall in the late fetal stages. To investigate a possible increased vulnerability to atherosclerosis in adulthood, we studied neointima formation in both groups after induction of lowered shear stress levels by perivascular constrictive collar placement around the carotid arteries.

Methods

Mice

The apoE$^{-/-}$ mice used were generated by homologous recombination in embryonic stem cells as described and backcrossed ≥8 times to a C57Bl/6J background.[8] Wild-type C57Bl/6J mice were purchased from Charles River Laboratories (Maastricht, The Netherlands, import agency for Jackson Laboratories). The apoE$^{-/-}$ and wild-type mice were crossbred to generate genetically identical apoE$^{+/-}$ fetuses (n=20 each group) from apoE$^{-/-}$ mothers (n=5) as well as from wild-type mothers (n=5). To examine the long-term effects of prenatal exposure to risk factors for atherosclerosis, we used female apoE$^{+/-}$ offspring (n=10 each group). After weaning (age 4 weeks), the animals received a Western-type diet (1% cholesterol, Hope Farms) for 16 weeks. Diet and water were provided ad libitum. The Committee on Animal Welfare, Leiden University Medical Center, approved all of the animal experiments.

Lipid Measurements

Total levels of cholesterol and triglycerides were enzymatically quantified in blood plasma of 4-hour fasted animals by using commercially available kits (Roche). Adult blood samples were obtained through tail bleeding. Maternal blood samples were acquired before pregnancy and at day 17.5 of pregnancy while fetal blood samples were acquired by decapitation at embryonic day 17.5 (E17.5). Samples of the offspring were acquired at the postnatal ages of 4, 8 and 16 weeks.

Carotid Collar placement

Neointima formation was induced in a random order by perivascular collar placement in apoE$^{+/-}$ offspring and C57BL/6J controls (n=5) at the age of 16 weeks as previously described.[9] Mice were anesthetized by intraperitoneal injection of Domitor (0.5 mg/kg, Pfizer), Dormicum (5 mg/kg, Roche) and Fentanyl (0.05 mg/kg, Janssen-Cilag). A constrictive silicone collar (0.31 mm ID, 0.64 mm OD, and 2.0 mm length, Helixmark) was placed around the left common carotid artery. After wound closing, anesthesia was antagonized with a subcutaneous injection of Antisedan (2.5 mg/kg, Pfizer), Anexate (0.5 mg/kg, Roche) and Naloxone (1.2 mg/kg).

Magnetic Resonance Microscopy

Visualization of the arterial tree was performed 4 weeks after collar placement. For detailed information on MRI see Appendix.

Tissue Harvesting and Preparation

At E17.5, fetal thorax tissue was removed and fixed in 4% paraformaldehyde in 0.1 mol/L of sodium phosphate buffer (pH 7.4) for 48 hours or embedded in TissueTek (Bayer) for nonfixated cryosections. Four weeks after collar placement, the mice were anesthetized and the thorax opened. Pressure-perfusion fixation (76 mm Hg) was performed through the cardiac left ventricle with PBS for 5 minutes followed by 4% paraformaldehyde in 0.1 mol/L of PHEM buffer (60 mmol/L of Pipes, 25 mmol/L of Hepes, 10 mmol/L of ethyleneglycoltetraacetic acid, and 2 mmol/L of $MgCl_2$; pH 6.97) for 5 minutes. The aorta and common carotid arteries were harvested and the collar was removed. Pressure-perfusion with only PBS was used for cryosections. The specimens were fixed for 48 and 6 hours, respectively, in 4% paraformaldehyde in 0.1 mol/L of PHEM buffer. After fixation, the tissue was dehydrated in ethanol and xylene and paraffin embedded. Transverse 5-µm sections were cut and serially mounted.

Immunohistochemistry

Routine staining was performed with hematoxylin and eosin, Resorcin-Fuchsin for detection of elastin, Sirius red for collagen, and Oil Red O to assess lipid deposition. Unless indicated otherwise, the immunohistochemistry was performed as described.[10] Sections were incubated overnight at room temperature with a mouse monoclonal primary antibody against α-smooth muscle actin to identify vascular smooth muscle cells (1:2000, Sigma Aldrich, Product No. A2547), a rat monoclonal anti-CD31 (1:50, PharMingen) and rabbit polyclonal anti-von Willebrand factor (vWF; 1:2000, DAKO) to study endothelial cells, and a rat monoclonal Mac-3 (1:400, PharMingen) against macrophages. Goat anti-rabbit biotin conjugate (1:200, Vector), goat anti-rat biotin conjugate (1:200, PharMingen), and rabbit anti-mouse peroxidase conjugate (1:200, DAKO) with normal goat and mouse serum diluted in PBS were used as secondary antibodies (1 hour at room temperature). Biotin labeling was followed by incubation with Vectastain ABC (Vector). The CD31 signal was enhanced with a colony-stimulating activity kit (DAKO). 3-3' Diaminobenzidine tetrahydrochloride was used as chromogen and counterstaining was performed with Mayer's hematoxylin.

Morphometry

To estimate the total volume of endothelial cells in the fetal carotid arteries at E17.5 the Cavalieri principle,[11] a point counting method using a grid, was used in 5 equally spaced sections stained with vWF (n=5 each group). In addition, morphometry was used to estimate the total volume of neointimal lesions in the

adult carotid artery. To exclude bias because of differences in maximum neointima area, the complete plaque was studied by volume measurements. Lumen and medial volume were also estimated. Contralateral noncompromised carotid arteries were assessed in a comparable region. Fifteen equally spaced sections were examined. The total intimal volume was measured between the endothelial cell monolayer and internal elastic lamina and total medial volume between the external and internal elastic lamina. The intima/media ratio was calculated by dividing the intimal volume by the medial volume.

Statistical Analysis

Data are represented as mean ± SEM. Paired and unpaired data were evaluated by 2-tailed Student's *t*-test. The differences were considered to be significant if $P < 0.05$.

Results

Lipid Metabolism

To study the effect of maternal hypercholesterolemia and associated risk factors on fetal lipid levels, we determined maternal and fetal plasma cholesterol and triglyceride levels. Maternal total plasma cholesterol and triglyceride levels are shown in Table 1. As expected, before and during pregnancy plasma cholesterol and triglyceride levels differed significantly between wild-type and apoE$^{-/-}$ mothers. Plasma cholesterol concentrations in both groups significantly decreased during pregnancy. A striking reduction of 51% was observed in plasma cholesterol levels of apoE$^{-/-}$ mothers at pregnancy day 17.5 but the cholesterol status remained hypercholesterolemic. Plasma triglyceride levels increased significantly in pregnant wild-type mothers, but not in the apoE$^{-/-}$ mothers.

Maternal hypercholesterolemia in apoE$^{-/-}$ mothers resulted in a significant plasma cholesterol elevation in apoE$^{+/-}$ mice at E17.5 compared with fetuses from wild-type mothers (Table 2). The plasma cholesterol levels found in apoE$^{+/-}$ offspring at weaning and in adult life after a Western-type diet were similar. Plasma triglyceride levels were low in all of the fetuses.

Table 1. Maternal plasma cholesterol and triglyceride levels

Mother	TC (mmol/L)	TG (mmol/L)
Wild-type		
Before pregnancy	1.98 ± 0.15	0.50 ± 0.03
Pregnancy day 17.5	1.33 ± 0.04*	1.58 ± 0.12*
ApoE$^{-/-}$		
Before pregnancy	20.13 ± 0.44‡	1.50 ± 0.10‡
Pregnancy day 17.5	9.42 ± 0.79*‡	2.08 ± 0.21‡

All data are shown as mean ± SEM. TC indicates total plasma cholesterol; TG, total plasma triglyceride. *$P < 0.05$ versus before pregnancy, ‡$P < 0.05$ versus other group at same time point.

Fetal Carotid Artery Composition

To examine the effect of intrauterine exposure to maternal atherosclerotic risk factors on fetal vascular remodeling, we studied the morphology of the vascular wall of the carotid arteries in apoE$^{+/-}$ fetuses from wild-type and apoE$^{-/-}$ mothers at E17.5. No fatty streaks were observed in the carotid arteries of all fetuses. However, in carotid arteries of fetuses from apoE$^{-/-}$ mothers increased endothelial cell damage was detected (Figure 1A). With light microscopic examination we

detected several areas in the carotid arteries where endothelial cells were absent. Morphometry revealed significantly less endothelial cell volume in the carotid arteries of apoE$^{+/-}$ fetuses from apoE$^{-/-}$ mothers compared with fetuses from wild-type mothers (18.81 ± 1.54x10^4 versus 24.81 ± 1.11x10^4 µm^3; Figure 1B). We found no lipid deposition in the vascular wall. In addition, Mac-3 staining showed that macrophages were not present in the vascular wall (results not shown). Overall quantification of vWF staining intensity in individual endothelial cells showed no significant difference between the two groups.

Table 2. Offspring plasma cholesterol and triglyceride levels

Mother	Offspring	TC (mmol/L)	TG (mmol/L)
Wild-type	**ApoE$^{+/-}$**		
	E17.5	1.54 ± 0.04	0.30 ± 0.01
	4 weeks	2.00 ± 0.03	0.93 ± 0.03
	8 weeks	6.21 ± 0.14	0.70 ± 0.02
	16 weeks	7.89 ± 0.31	0.44 ± 0.02
ApoE$^{-/-}$	**ApoE$^{+/-}$**		
	E17.5	2.11 ± 0.06*	0.37 ± 0.02
	4 weeks	1.90 ± 0.06	0.81 ± 0.05
	8 weeks	7.08 ± 0.21	0.56 ± 0.04
	16 weeks	7.73 ± 0.36	0.47 ± 0.02

All data are shown as mean ± SEM. TC indicates total plasma cholesterol; TG, total plasma triglyceride. *P < 0.000 at E17.5 versus other group at the same time point.

Carotid Artery Visualization by MRI

Four weeks after collar placement, the carotid arteries and the position of the collar could clearly be visualized with magnetic resonance microscopy in all of the C57BL/6J mice (Figure 2A). In 4 of 5 apoE$^{+/-}$ mice born from wild-type mothers, the angiography revealed a normal carotid artery lumen proximal to the position of the collar (Figure 2B). In 1 case the left carotid artery could not be visualized as a result of thrombus formation within the collar (confirmed by histology). In the group of apoE$^{+/-}$ mice from apoE$^{-/-}$ mothers, only 1 angiography resembled the wild-type. In 2 cases the lumen of the left carotid artery was only partly visualized, whereas in the other 2 mice the left carotid artery lumen was completely absent (Figure 2C). Histology revealed that the lack of visualization was caused by severe lumen narrowing as a result of presence of intimal thickening proximal to the collar.

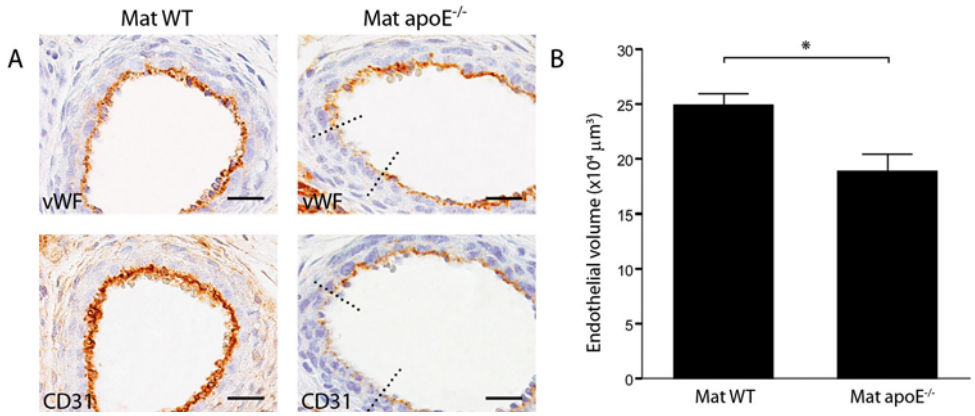

Figure 1. Effects of in utero exposure of apoE$^{+/-}$ fetuses to maternal atherosclerotic risk factors on endothelial cells of the carotid arteries. (A) Representative immunostaining for vWF and CD31 in cross-sections from apoE$^{+/-}$ fetuses from wild-type (Mat WT, left panels) and apoE$^{-/-}$ mothers (Mat apoE$^{-/-}$, right panels) at age E17.5. Region between broken lines indicates an area of decreased expression of vWF and CD31, respectively. Scale bars, 20 µm. (B) Morphometric analysis of endothelial cell volume in the carotid arteries. Data are mean ± SEM (n=5 each). *P < 0.01.

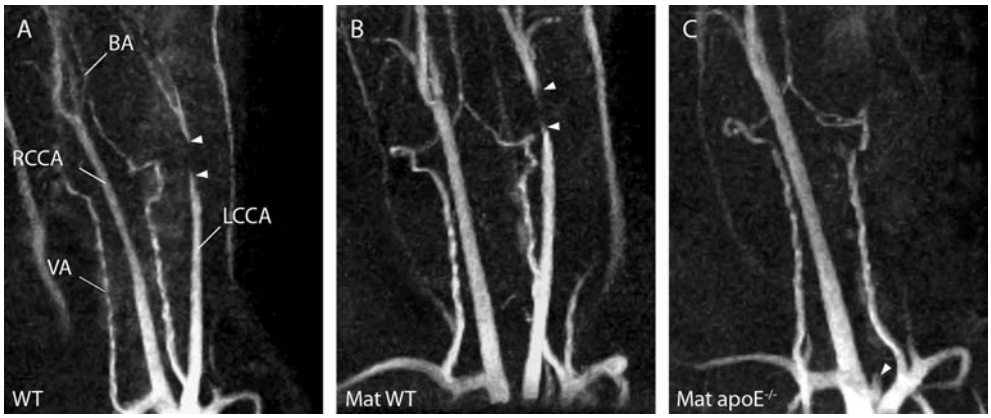

Figure 2. Effects of a constrictive collar four weeks after placement around the left common carotid artery. Angiographies representative for 20 weeks old (A) wild-type (WT), (B) apoE$^{+/-}$ from wild-type mothers (Mat WT) and (C) apoE$^{+/-}$ mice from apoE$^{-/-}$ mothers (Mat apoE$^{-/-}$). The induced intimal thickening in Mat apoE$^{-/-}$ reduces the flow to an undetectable level, only the trunk of the LCCA is visible. BA indicates basilar artery; VA, vertebral artery; RCCA, right common carotid artery; LCCA, left common carotid artery. Arrows indicate the region of the collar and in (C) the trunk of the LCCA.

Lesion Size

Spontaneous neointima formation was assessed in adult apoE$^{+/-}$ offspring from wild-type and apoE$^{-/-}$ mothers at the age of 20 weeks. No lesions were detected at the level of the aortic root and in the aortic arch (see Appendix). In addition, in noncompromised carotid arteries normal vascular wall morphology was observed (Figure 3A). We found that collar placement resulted in severe neointima formation proximal to the collar in apoE$^{+/-}$ mice from apoE$^{-/-}$ mothers (9 of 10) compared with minor lesions in the offspring from wild-type mothers (2 of 10) (Figure 3B-C). Significantly increased lesion volume was observed in offspring of apoE$^{-/-}$ mothers ($5.04 \pm 1.65 \times 10^6$ versus $0.28 \pm 0.18 \times 10^6$ μm^3; $P = 0.018$; Figure 4A). A trend towards increased medial volume was observed as result of collar placement (Figure 4B). A significant increase in medial volume was detected between the noncompromised and the collared carotid arteries of in utero exposed apoE$^{+/-}$ mice ($20.34 \pm 0.77 \times 10^6$ versus $29.96 \pm 2.56 \times 10^6$ μm^3; $P = 0.04$). Medial volumes between the contralateral arteries of both groups did not differ. The intima/media ratio was significantly increased in apoE$^{+/-}$ mice from apoE$^{-/-}$ mothers (0.15 ± 0.05 versus 0.01 ± 0.01; $P = 0.017$; Figure 4C). Severe lesions were characterized by a cylindrical structure and maximal intima/media ratios of ≈ 1.0.

Lesion Composition

To assess the role of several cell lineages in intimal proliferation, neointimal lesion composition was studied. The endothelial cell lining was, in contrast to the findings in the fetuses, in all cases intact (Figure 5A). The vWF was absent in the endothelial cells and present subendothelially (Figure 5B). All lesions contained macrophages (Figure 5C). Extensive extracellular matrix deposition was demonstrated throughout the neointima by increased presence of elastin and collagen (Figure 5D-E). Enhanced medial volume in collared arteries appeared also to be the result of increased collagen production. All elastic lamina of the media were intact, thereby excluding major invasion of medial smooth muscle cells into the intima at this stage. Staining for α-smooth muscle actin was not restricted to the media, but positive cells were also detected in the intima (Figure 5F).

Oil red O staining revealed that Western-type diet alone did not result in lipid deposition in the carotid arteries (Figure 6A). A second trigger, collar placement, resulted in limited accumulation of lipids in the media only directly proximal to the collar in apoE$^{+/-}$ mice from wild-type mothers (Figure 6B). On the contrary, massive lipid deposition was observed in the intima as well as in the media of collared arteries of apoE$^{+/-}$ mice from apoE$^{-/-}$ mothers (Figure 6C).

The vascular wall of all contralateral, noncompromised carotid arteries showed a normal morphology. In addition to immunohistochemical analysis of these arteries, we performed microarray analysis to detect changes in intrinsic gene expression patterns (see Appendix for preliminary data).

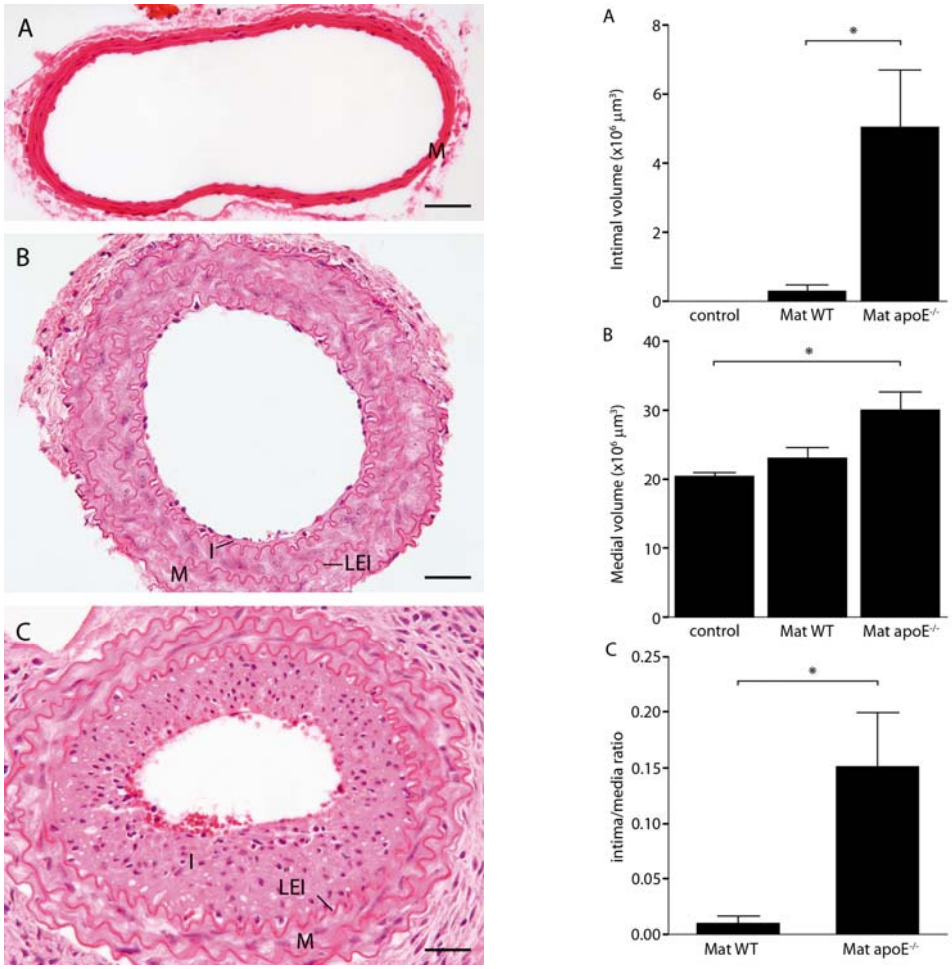

Figure 3. Morphology of adult carotid arteries. Mice were euthanized at 20 weeks of age, 4 weeks after collar placement. Perfusion-fixation induced dilatation of the arteries. Presence of intimal thickening prevented dilatation. Representative HE staining in cross-sections from (A) noncompromised carotid arteries and the region proximal to the collar in apoE$^{+/-}$ mice from (B) wild-type and (C) apoE$^{-/-}$ mothers, respectively. I indicates intima; M, media; LEI, lamina elastica interna. Scale bars: 30 µm.

Figure 4. Morphometric analysis of the effects of collar placement. (A) Estimation of intimal volume and (B) medial volume of noncompromised (control) and collared carotid arteries of apoE$^{+/-}$ mice from wild-type (Mat WT) and apoE$^{-/-}$ (Mat apoE$^{-/-}$) mothers. (C) Calculated intima/media ratio for the collared carotid arteries of both apoE$^{+/-}$ groups. Data are mean ± SEM (n=10 each). *P < 0.05.

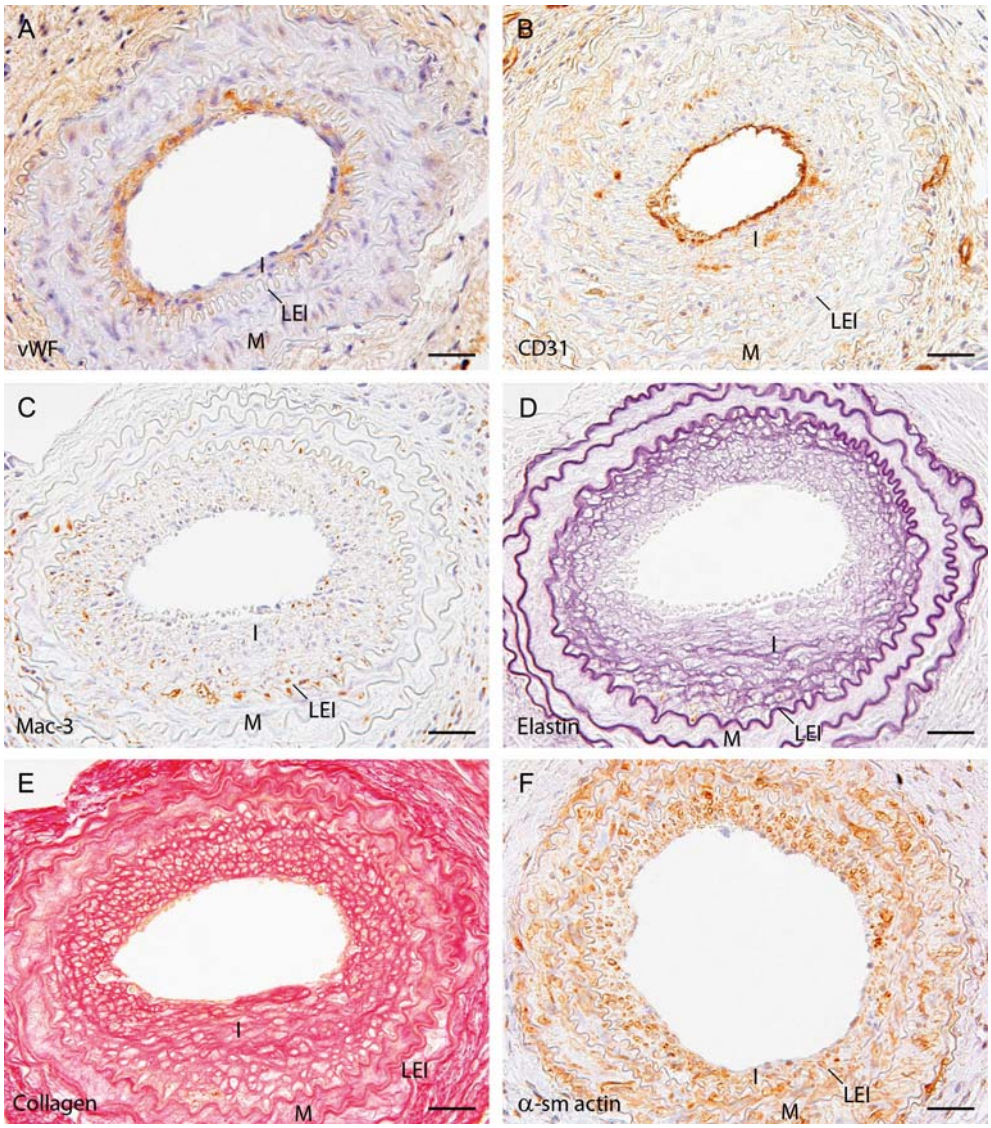

Figure 5. Neointima composition. Representative cross-sections from apoE$^{+/-}$ mice from apoE$^{-/-}$ mothers were stained to study (A and B) endothelial cells, (C) macrophages, (D and E) extracellular matrix production and (F) α-sm actin expression. I indicates intima; M, media; LEI, lamina elastica interna. Scale bars: 30 μm.

Figure 6. Oil Red O staining. Representative staining in cross-sections from (A) noncompromised carotid arteries and the region proximal to the collar in apoE$^{+/-}$ mice from (B) wild-type and (C) apoE$^{-/-}$ mothers. The collar induces deposition of lipids in the media in the low flow areas in B. Note the increase in lipid deposition in the Mat apoE$^{-/-}$ offspring in C. I indicates intima; M, media; LEI, lamina elastica interna; L, lumen. Scale bars, 30 μm. ➡

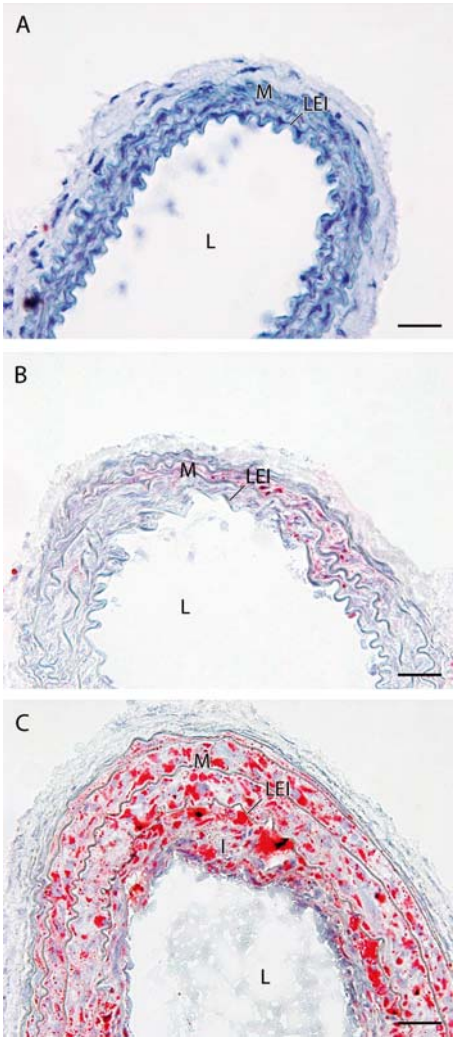

Discussion

The present study has provided evidence that the susceptibility to atherosclerosis of morphologically normal adult vessels can already be imprinted during prenatal development. We showed that in utero exposure of apoE$^{+/-}$ embryos and fetuses to environmental maternal atherosclerotic risk factors can prime the vasculature to severely aggravated neointima formation in morphological normal adult carotid arteries after collar placement compared with nonexposed offspring from wild-type mothers. In apoE$^{+/-}$ mice the remaining apoE allele is sufficient to generate plasma apoE levels equal to those of wild-type animals (reviewed by Getz and Reardon[12]). Furthermore, plasma lipid levels of both groups of mice are indistinguishable when fed chow or a moderate Western-type diet,[7,8] and spontaneous atherosclerosis development in the aortic root is absent. Homozygous apoE-deficiency in mice is associated with hypercholesterolemia,[5,6] increased oxidative stress levels,[13] and enhanced inflammatory status,[14] and all of these factors may have a role in the process of programming of the vessel wall of apoE$^{+/-}$ offspring. However, contribution of other factors associated with apoE-deficiency cannot be excluded.

Because apoE-deficiency is associated with hypercholesterolemia, we assessed the effect of increased maternal cholesterol status on fetal cholesterol levels. In our analysis we found that maternal hypercholesterolemia enhanced fetal plasma cholesterol levels. Neonatal plasma cholesterol levels did not differ between apoE$^{+/-}$ mice from apoE$^{-/-}$ and wild-type mothers. Our data are in concordance with previous studies in humans, rats, and mice that demonstrated that no correlation exists between maternal and fetal plasma cholesterol levels late in pregnancy and at and after birth.[1,15-17] However, we have no data available on fetal plasma cholesterol levels earlier in pregnancy. Because several reports

indicate that, during mid-pregnancy, fetal plasma cholesterol levels are very high,[1,18] the slight significant difference observed at E17.5 may be a reflection of larger differences earlier in development.

Studies in human subjects revealed that fatty streaks are present in fetal aortas and carotid arteries, and the existence of maternal hypercholesterolemia throughout pregnancy leads to an increased number and size of the lesions.[1,19] In human cerebral and coronary arteries on the other hand, no lipid accumulations and macrophages were detected prenatally.[19,20] In rabbits, diet-induced maternal hypercholesterolemia results in extensive lesion formation in the aorta of the offspring at birth.[3] Our data show that the presence of maternal atherosclerotic risk factors leads to endothelial cell activation and damage in carotid arteries of apoE$^{+/-}$ fetuses. Except for these early markers of atherosclerosis,[21] no morphological abnormalities, e.g. fatty streaks, were observed in the murine fetal carotid arteries.

Furthermore, no intimal thickening was detected in the aorta of the fetuses (unpublished data). Anatomical and functional differences in arteries, as well as discrepancies between species, may explain the observed distinction in atherosclerotic lesion formation in fetal life. Because apoE$^{+/-}$ mice from apoE$^{-/-}$ mothers lack atherosclerotic lesions in fetal vasculature and spontaneous lesion formation in the aortic root, aortic arch, and carotid arteries at the age of 20 weeks, our model is very useful to study the long-term consequences of imprinting of morphologically normal vessels.

ApoE-deficiency leads to high levels of reactive oxygen species in the circulation and tissues.[22] In addition, it has been described that atherosclerosis development in these mice is accompanied by a reduction in antioxidant enzymes in the athero-prone areas.[23] It has been suggested that reactive oxygen species pass the placenta[24] and as a result may influence the oxidative status of the fetus. Napoli and colleagues[3] and Palinski and colleagues[25] reported that addition of vitamin E or cholestyramine to the diet of rabbits significantly diminished atherosclerosis in the offspring. Oxidative stress has also been described to affect DNA methylation.[26,27] As a consequence, embryonic development, as well as other physiological processes may be modulated by increased oxidative stress. We hypothesize that maternal hypercholesterolemia through oxidative stress affects signaling processes in the cell lineages of the fetal vascular wall and bone marrow leading to functional changes in these cells. That epigenetic changes are likely to be responsible for the aggravated atherogenic response to collar-induced shear stress changes in adult life is currently a focus of our ongoing investigations.

There seems to be a paradox between our study and a previous study by Madsen and colleagues[15] who did not observe an effect of in utero exposure to maternal atherosclerotic risk factors on atherosclerotic lesion formation in adult life.

In the latter study, spontaneous lesion formation was induced by a Western-type diet containing the strong atherosclerosis-inducing factor cholate. In long-term survivors, they detected equal degrees of advanced atherosclerosis. In our study, spontaneous expression of atherosclerosis was missing, and we studied the initial stages of neointima formation, which turned out to be different between the two groups of apoE$^{+/-}$ mice. Therefore, our studies cannot be reliably compared.

The striking differences in adult lesion formation between the in utero exposed and nonexposed apoE$^{+/-}$ mice raise the question which cell types involved are affected during embryonic development. The most obvious vascular cell populations to be considered are the endothelial and smooth muscle cells of the carotid arteries and the circulating bone marrow-derived cells. Changes in the gene expression profiles of mural cells after in utero exposure to high cholesterol levels has been recently demonstrated in Ldlr$^{-/-}$ mice.[4] Diet-induced maternal hypercholesterolemia in Ldlr$^{-/-}$ mothers significantly altered the expression of 139 genes in descending aortas of Ldlr$^{-/-}$ offspring without signs of lesion formation. These data are in line with our gene set enrichment analysis of the microarray data of noncompromised carotid arteries showing changes in gene expression as a result of in utero exposure to maternal atherosclerotic risk factors (see Appendix). This method allows insight into the dynamics of genes contributing to a gene set without having to work within the fixed thresholds that genes have to meet to be differentially expressed and demonstrated altered regulations of various pathways in the vascular wall. Larger sample sizes of carotid arteries and descending aortas in combination with laser dissection microscopy will give us insight into the vulnerability of the individual cell populations for induction of changes in gene expression as a consequence of prenatal exposure to atherosclerotic risk factors.

In conclusion, the present study has provided evidence that the susceptibility to atherosclerosis of morphologically normal adult vessels is already imprinted during prenatal development and is not genetically determined in our model. In the presence of additional risk factors, neointima formation in adult life is severely accelerated. Our findings indicate that the basis for development of atherosclerosis in adult life is already laid down during embryonic development. Risk factors for atherosclerosis in human adults are mainly associated with lifestyle. Extensive lifestyle management can, thus, reduce the number of environmental triggers that induce aggravated atherosclerotic lesion formation. Future research will concentrate on the mechanisms involved in the priming process, as well as on prevention strategies.

Acknowledgements

We are grateful to Jan Lens for his graphic support, Klaas Koop and Bert Wisse for their help with the vWF quantification and morphometric analyses, and Ulrike Nehrdich and colleagues for animal care and breeding. We also thank the Center for Medical System Biology, established by the Netherlands Genomics Initiative/Netherlands Organization for Scientific research, and the Nutrigenomics Consortium. F.E.A. and A.E.S. are supported by grants from the Netherlands Heart Foundation (2003B241 and 2001B141).

Reference List

1. Napoli C, D'Armiento FP, Mancini FP, Postiglione A, Witztum JL, Palumbo G, Palinski W. Fatty streak formation occurs in human fetal aortas and is greatly enhanced by maternal hypercholesterolemia. Intimal accumulation of low density lipoprotein and its oxidation precede monocyte recruitment into early atherosclerotic lesions. *J Clin Invest.* 1997;100:2680-2690.
2. Napoli C, Glass CK, Witztum JL, Deutsch R, D'Armiento FP, Palinski W. Influence of maternal hypercholesterolaemia during pregnancy on progression of early atherosclerotic lesions in childhood: Fate of Early Lesions in Children (FELIC) study. *Lancet.* 1999;354:1234-1241.
3. Napoli C, Witztum JL, Calara F, de Nigris F, Palinski W. Maternal hypercholesterolemia enhances atherogenesis in normocholesterolemic rabbits, which is inhibited by antioxidant or lipid-lowering intervention during pregnancy - An experimental model of atherogenic mechanisms in human fetuses. *Circ Res.* 2000;87:946-952.
4. Napoli C, de Nigris F, Welch JS, Calara FB, Stuart RO, Glass CK, Palinski W. Maternal hypercholesterolemia during pregnancy promotes early atherogenesis in LDL receptor-deficient mice and alters aortic gene expression determined by microarray. *Circulation.* 2002;105:1360-1367.
5. Plump AS, Smith JD, Hayek T, Aalto-Setala K, Walsh A, Verstuyft JG, Rubin EM, Breslow JL. Severe hypercholesterolemina and atherosclerosis in apolipoprotein e-deficient mice created by homologous recombination in ES cells. *Cell.* 1992;71:343-353.
6. Zhang SH, Reddick RL, Piedrahita JA, Maeda N. Spontaneous hypercholesterolemia and arterial lesions in mice lacking apolipoprotein E. *Science.* 1992;258:468-471.
7. Bobkova D, Honsova E, Kovar J, Poledne R. Effect of diets on lipoprotein concentrations in heterozygous apolipoprotein E-deficient mice. *Physiol Res.* 2004;53:635-643.
8. Van Ree JH, van den Broek WJ, Dahlmans VE, Groot PH, Vidgeon-Hart M, Frants RR, Wieringa BA. Diet-induced hypercholesterolemia and atherosclerosis in heterozygous apolipoprotein E-deficient mice. *Atherosclerosis.* 1994;111:25-37.
9. Von der Thüsen JH, van Berkel TJ, Biessen EA. Induction of rapid atherogenesis by perivascular carotid collar placement in apolipoprotein E-deficient and low-density lipoprotein receptor-deficient mice. *Circulation.* 2001;103:1164-1170.
10. Bergwerff M, Verberne ME, DeRuiter MC, Poelmann RE, Gittenberger-de Groot AC. Neural crest cell contribution to the developing circulatory system. Implications for vascular morphology? *Circ Res.* 1998;82:221-231.
11. Gundersen HJ, Jensen EB. The efficiency of systematic sampling in stereology and its prediction. *J Microscopy.* 1987;147:229-263.
12. Getz GS, Reardon CA. Diet and murine atherosclerosis. *Arterioscler Thromb Vasc Biol.* 2006;26:242-249.
13. Hayek T, Oiknine J, Brook JG, Aviram M. Increased plasma and lipoprotein lipid peroxidation in apo E-deficient mice. *Biochem Biophys Res Commun.* 1994;201:1567-1574.
14. Grainger DJ, Reckless J, McKilligin E. Apolipoprotein E modulates clearance of apoptotic bodies in vitro and in vivo, resulting in a systemic proinflammatory state in apolipoprotein E-deficient mice. *J Immunol.* 2004;173:6366-6375.
15. Madsen C, Dagnaes-Hansen F, Moller J, Falk E. Hypercholesterolemia in pregnant mice does not affect atherosclerosis in adult offspring. *Atherosclerosis.* 2003;168:221-228.
16. De Assis SM, Seguro AC, Helou CM. Effects of maternal hypercholesterolemia on pregnancy and development of offspring. *Pediatr Nephrol.* 2003;18:328-334.

17. Munilla MA, Herrera E. A cholesterol-rich diet causes a greater hypercholesterolemic response in pregnant than in nonpregnant rats and does not modify fetal lipoprotein profile. *J Nutr.* 1997;127:2239-2245.
18. McConihay JA, Horn PS, Woollett LA. Effect of maternal hypercholesterolemia on fetal sterol metabolism in the Golden Syrian hamster. *J Lipid Res.* 2001;42:1111-1119.
19. Napoli C, Witztum JL, de Nigris F, Palumbo G, D'Armiento FP, Palinski W. Intracranial arteries of human fetuses are more resistant to hypercholesterolemia-induced fatty streak formation than extracranial arteries. *Circulation.* 1999;99:2003-2010.
20. Ikari Y, McManus BM, Kenyon J, Schwartz SM. Neonatal intima formation in the human coronary artery. *Arterioscler Thromb Vasc Biol.* 1999;19:2036-2040.
21. Davignon J, Ganz P. Role of endothelial dysfunction in atherosclerosis. *Circulation.* 2004;109:III27-III32.
22. Ohara Y, Peterson TE, Harrison DG. Hypercholesterolemia increases endothelial superoxide anion production. *J Clin Invest.* 1993;91:2546-2551.
23. 't Hoen PA, Van der Lans CA, van Eck M, Bijsterbosch MK, van Berkel TJ, Twisk J. Aorta of ApoE-deficient mice responds to atherogenic stimuli by a prelesional increase and subsequent decrease in the expression of antioxidant enzymes. *Circ Res.* 2003;93:262-269.
24. Fantel AG, Mackler B, Stamps LD, Tran TT, Person RE. Reactive oxygen species and DNA oxidation in fetal rat tissues. *Free Radic Biol Med.* 1998;25:95-103.
25. Palinski W, D'Armiento FP, Witztum JL, de Nigris F, Casanada F, Condorelli M, Silvestre M, Napoli C. Maternal hypercholesterolemia and treatment during pregnancy influence the long-term progression of atherosclerosis in offspring of rabbits. *Circ Res.* 2001;89:991-996.
26. Wachsman JT. DNA methylation and the association between genetic and epigenetic changes: relation to carcinogenesis. *Mutat Res.* 1997;375:1-8.
27. Weitzman SA, Turk PW, Milkowski DH, Kozlowski K. Free radical adducts induce alterations in DNA cytosine methylation. *Proc Natl Acad Sci U S A.* 1994;91:1261-1264.

Appendix

Methods

Magnetic Resonance Microscopy

Mice were imaged in vivo using a vertical 9.4T (400 MHz), 89 mm bore magnet with a shielded 1T/m gradient and a transmit/receive birdcage radiofrequency coil with an inner diameter of 30 mm (Bruker Biospin, Rheinstetten, Germany). Bruker ParaVision 3.02 software was used for image acquisition and analysis. Mice (n=5 each group) were initially anesthetized with 4% isoflurane (Abbott, Hoofddorp, The Netherlands) in air (0.3 l min^{-1}) and O_2 (0.3 l min^{-1}) and maintained with ~1.5% isoflurane during all procedures. Anesthetized mice were mounted into a probehead and inserted head-up into the magnet. The respiratory rate was monitored via an air-pressure cushion connected to a laptop using Biotrig software (Bruker, Rheinstatten, Germany). The depth of the anesthesia was continuously regulated to maintain a stable respiration rate during the experiment. We used a 3D FLASH (fast low angle shot) sequence with an echo time of 1.85 ms, a repetition time of 30 ms, a 0.8 ms sinc radio frequency pulse with a flip angle of 30 degrees and a spectral band width of 100 kHz. With a field of view (FOV) of 20x20x20 mm, a matrix of 256x256x256 an isotropic resolution of 78 µm was reached within a scan time of 32 minutes and 46 seconds. 3D angiograms were generated in ParaVision by maximum intensity projection.

Microarray

Total RNA was isolated from noncompromised contralateral carotid arteries at the age of 20 weeks of 3 $apoE^{+/-}$ offspring from wild-type mothers and 4 offspring from $apoE^{-/-}$ mothers. RNA was isolated with the RNAqueous® Micro Kit (Ambion, Cambridgeshire, UK) according to the manufacturers protocol. The RNA concentration was determined by absorbency at 260 nm with a NanoDrop (Isogen Life Science B.V., IJsselstein, The Netherlands) and RNA integrity was verified by use of the RNA 6000 Pico assay on a Agilent 2100 Bioanalyzer (Agilent Technologies, Amstelveen, The Netherlands). All of the RNA was subjected to a first round of oligo-dT primed amplification with the MessageAmp™II aRNA Amplification Kit (Ambion). One µg of aRNA was used in a random primed second round of amplification (MessageAmp™II-Biotin Enhanced Kit, Ambion) to obtain biotin labeled aRNA. Hybridization, washing and scanning of mouse genome 430A GeneChip arrays (Affymetrix) was performed according to Affymetrix standard

protocols (http://www.affymetrix.com). After scanning, the images were quantified using the Affymetrix GeneChip Operating software. The scaled data were then imported into the R software environment (http://www.R-project.org) and analyzed with the Bioconductor (http://www.bioconductor.org) R/affy package. Normalization was performed by the Robust Multi-array Average method.[1] Gene expression levels were analyzed with the R/limma package (http://www.bioconductor.org) and corrected for multiple testing by false discovery rate (FDR) according to Benjamini and Hochberg.[2]

Results

Spontaneous Atherosclerosis

ApoE$^{+/-}$ mice only develop atherosclerosis when fed a high fat Western-type diet. To examine the extent of spontaneous lesion development in our mouse model, the aortas of the apoE$^{+/-}$ mice from apoE$^{-/-}$ and wild-type mothers were examined at the termination of the experiment, at the age of 20 weeks. No atherosclerotic lesions were observed at the level of the aortic root (Figure 1A). Furthermore, no lesions were observed in the aortic arch and at the bifurcations (Figure 1B).

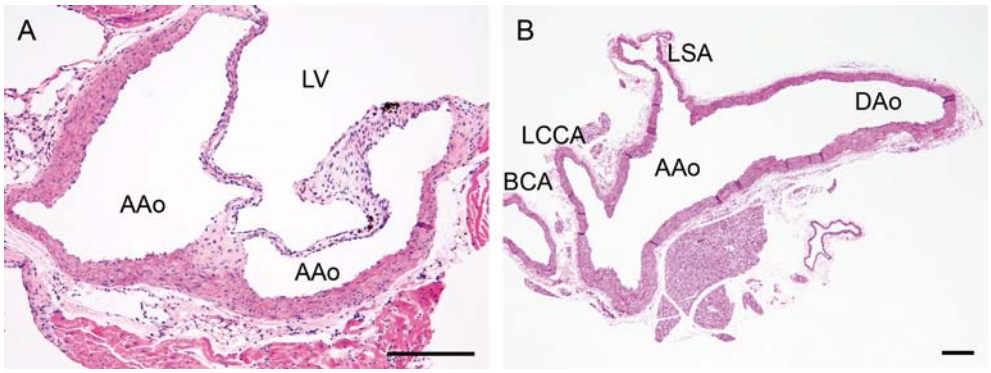

Figure 1. Analysis of spontaneous atherosclerosis. Pictures representative for (A) aortic root and (B) aortic arch. No lesions detectable. AAo indicates ascending aorta; LV, left ventricle; BCA, brachiocephalic artery; LCCA, left common carotid artery; LSA, left subclavian artery; AoA, aortic arch; DAo, dorsal aorta. Scale bars: (A) 200 µm and (B) 300 µm.

Gene Expression

Given the effect of intrauterine exposure to atherosclerotic risk factors on fetal carotid arteries and atherosclerotic lesion formation in adult life, we performed microarray analysis on the noncompromised carotid arteries of the apoE$^{+/-}$ mice from both wild-type and apoE$^{-/-}$ mothers to detect changes in intrinsic gene expression patterns. Up to 3309 genes had an unadjusted *P*-value of < 0.05 and 626 an unadjusted *P*-value of < 0.01. After correction for multiple testing no differentially expressed genes were detected. To exclude the possibility that relevant biological differences were not detected due to the relative noise inherent to the microarray technology, a gene set enrichment analysis was performed.[3] This analysis revealed a number of upregulated pathways among which the CTLA-4 and TCRA T-cell activating pathway, the pro-inflammatory IL-12/STAT-4 pathway as well as pathways involved in fatty acid and the carbohydrate metabolism

(Table 1). The complete microarray analysis is available at http://www.ncbi.nlm.nih.gov/geo/, query GSE6134. Although the amount of samples available for the microarray analysis was limited, the nominal *P*-value was significant for the top ranked pathways. Therefore, the results may give rise to hypotheses for future research.

Table 1. Top ranked pathways gene set enrichment analysis.

ID	Pathway	nominal *P*-value
1	TCA	**0.000**
2	MAP00190_Oxidative_phosporylation	**0.000**
3	FA	**0.000**
4	Krebs-TCA_Cycle	**0.000**
5	GO_0005739	**0.000**
6	TcytotoxicPathway	**0.037**
7	CR_immune_function	**0.038**
8	TcraPathway	**0.040**
9	Ctla4Pathway	**0.040**
10	Il17Pathway	**0.042**
11	Tob1Pathway	**0.043**
12	IL12Pathway	**0.047**
13	No2il12Pathway	**0.049**

Nominal *P*-value = *P*-value without correction for multiple testing.

Reference List

1. Irizarry RA, Hobbs B, Collin F, Beazer-Barclay YD, Antonellis KJ, Scherf U, Speed TP. Exploration, normalization, and summaries of high density oligonucleotide array probe level data. *Biostatistics.* 2003;4:249-264.
2. Benjamini Y, Hochberg Y. Controlling the false discovery rate: a practical and powerful approach to multiple testing. *J Roy Statist Soc Ser.* 2006;B 57:289-300.
3. Subramanian A, Tamayo P, Mootha VK, Mukherjee S, Ebert BL, Gillette MA, Paulovich A, Pomeroy SL, Golub TR, Lander ES, Mesirov JP. Gene set enrichment analysis: a knowledge-based approach for interpreting genome-wide expression profiles. *Proc Natl Acad Sci U S A.* 2005;102:15545-15550.